Feasibility of the electrochemical way in molten fluorides for separating Thorium and Lanthanides and extracting Lanthanides from the solvent.

Pierre Chamelot, Laurent Massot, Céline Hamel, Christophe Nourry, Pierre Taxil

Feasibility of the electrochemical way in molten fluorides for separating Thorium and Lanthanides and extracting Lanthanides from the solvent.

P. Chamelot, L. Massot, C.Hamel, C. Nourry and P.Taxil

Laboratoire de Génie Chimique (LGC), Département Procédés Electrochimiques, CNRS-UMR 5503, Université Paul Sabatier, 31062 Toulouse Cedex 9, France.

Abstract: An alternative way of reprocessing nuclear fuel by hydrometallurgy could be using treatment with molten salts, particularly fluoride melts. Moreover, one of the six concepts chosen for GEN IV nuclear reactors (Technology Roadmap – http://gif.inel.gov/roadmap/) is the Molten Salt Reactor (MSR). The originality of the concept is the use of molten salts as liquid fuel and coolant. During the running of the reactor, fission products, particularly lanthanides, accumulate in the melt and have to be eliminated to optimise reactor operation.

This study concerns the feasibility of the separation actinides-lanthanides-solvent by selectively electrodepositing the elements to be separated on an inert (Mo, Ta) or a reactive (Ni) cathodic substrate in molten fluoride media.

The main results of this work lead to the conclusions that:

* The solvents to be used for efficient separation must be fluoride media containing lithium as cation.

* Inert substrates are suitable for actinide/lanthanide separation; nickel substrate is more suitable for the extraction of lanthanides from the solvent, owing to the depolarisation occurring in the cathodic process through alloy formation.

Keywords: molten fluorides, lanthanides, actinides, electrochemical separation, alloy formation.

1. Introduction

Up to now, the reprocessing of nuclear fuels has been carried out by hydrometallurgy (the PUREX Process). However, in long term strategies on the nuclear fuel cycling, this process may not be very appropriate for the reprocessing of future nuclear fuels, which will contain large amounts of transuranium elements and an inert matrix for tight confinement of radionucleide.

An alternative way to reprocess nuclear fuel would be the use of molten salts and particularly fluoride melts. The advantages are that they are not sensitive to radiolytic degradation, and are good solvents for the dissolution of the fuel. They thus open a large electrochemical window owing to their chemical stability.

For these reasons, the molten salt reactor concept was developed between 1954 and 1976 at Oak Ridge National Laboratory (ORNL) [1]. The main originality of this reactor's concept is the use of molten salt both as the fuel (U/Th cycle) and as the coolant. However, the reprocessing methodology was not developed and thus remains to be optimised.

The present study addresses the separation actinide-lanthanide-solvent by an electrochemical process that could be suitable for MSR reprocessing.

The methodology consists of selectively electrodepositing the element to be separated. The feasibility of the methodology is examined here in the following steps.

First, a thermodynamic investigation is presented which defined the nature and the composition of the fluoride media suitable for the separation. Then the electrochemical behaviour of each element involved in the separation (Th as actinide and Sm, Gd and Nd as lanthanides) was studied on inert electrodes (Mo or Ta) to determine the mechanism of reduction of these elements into metal and then to estimate the possibility of extraction of actinides from the molten media using the comparison of experimental data on the difference of the respective potentials of electrodeposition of the elements to be separated or extracted from the melt.

Finally, in order to facilitate the separation or extraction process, the use of a reactive electrode (Ni) leading to the formation of alloys was attempted to promote a depolarisation effect.

Based on cyclic voltammetry studies, the comparison of the reduction potentials of each element on the reactive electrode and on inert electrodes shows that the use of an inert cathode does improve the separation process.

Then, electrolysis was carried out on a nickel cathode to validate the feasibility of separations using this type of electrode.

2. Experimental

• The cell was a cylindrical refractory steel vessel, closed by a stainless steel lid with circulating water for cooling and placed under inert argon atmosphere (LINDE U quality, less than 5 ppm O_2) from which moisture and oxygen are removed using a purification cartridge (Air Liquide) [2-3].

• The salt mixture was placed in a vitreous carbon crucible (Carbone LorraineV25 grade) inside the vessel.

• The electrolytic bath was composed of a eutectic LiF/CaF_2 (Merck 99.99%) mixture (77/23 molar ratio). Solutes were introduced into the bath in the form of fluoride salt powders: SmF_3 (Merck 99.99%), GdF_3 (Merck 99.99%) NdF_3 (Merck 99.99%) and ThF_4 (CERAC 99.99%)).

• Experiments were performed in the temperature range 800-900°C.

• Molybdenum, tantalum and nickel wires (Goodfellow purity 99.99%, 1mm diameter) are used as working electrodes. Molybdenum and tantalum are inert with the studied elements whereas nickel can form alloys with them in the temperature range considered.

• The auxiliary electrode was a vitreous carbon (Carbone LorraineV25 grade) rod with a large surface area (2.5 cm²). The potentials are referred to a platinum wire (0.5mm diameter) acting as a quasi-reference electrode (QRE) $Pt/PtO_x/O^{2-}$ sensitive to only the oxide content in the bath [4].

• Cyclic voltammetry, chronopotentiometry and square-wave voltammetry are used for the investigation of the reduction process of the Sm, Gd, Nd and Th ions, and performed with an Autolab PGSTAT30 potentiostat/galvanostat controlled by a computer using the GPES 4.9 software.

• Techniques for the characterisation of reduction products: after the electrolysis runs, the surface of the cathodes was observed by scanning electron microscope (LEO 435 VP) and analysed with an EDS probe (Oxford INCA 200).

3. Results and discussion

3.1 Separation An / Ln / solvent by electrodeposition on an inert cathode

3.1 1 Selection of the solvent

Table 1 displays the standard potentials converted from the Gibbs energy data of the pure solid compounds from references [5, 6] and referred to the fluorine electrode (F_2/F^-). In the case of binary mixtures, considered as ideal, the activity of each compound is equal to its molar fraction; the calculation of the reduction potential of the least stable cations of the

solvent lead us to identify the solvent with the largest electroactive window, suitable for the reduction of the elements studied.

Table 1 helps to predict the reduction potential of the cation of each solvent and to compare it with the reduction of each compound studied. The data reported demonstrate that the reduction of LiF-CaF_2 or pure LiF proceeded at more cathodic potentials than the actinide and lanthanides (except samarium) studied here and can be used as solvent for performing the electrodeposition of pure Nd, Gd or Th.

According to these data, Sm metal cannot be extracted from any of these melts.

The LiF-CaF_2 binary mixture is preferred in this work to pure LiF owing to a lower melting point.

Remark: For the electrochemical reprocessing, the molten salt composed of LiF and BeF_2, which is cited as candidate for the MSR carrier melt, is not suitable because of its narrower electrochemical window (see in table 1).

3.1.2 Theoretical estimation of difference of potential necessary for a given efficiency of separation

The difference between the reduction potential of the elements to be separated depends on both the number of electrons exchanged to produce metal on the electrode and the desired separation rate.

The separation rate η can be defined by equation (1):

$$\eta = 1 - \frac{a_{final}}{a_{initial}} \qquad (1)$$

a_{final} and $a_{initial}$ are the molality of the element respectively before and after the separation or the extraction.

The theoretical difference of potential is determined writing Nernst's law for each element to be extracted with the initial and final concentrations:

$$\Delta E = E_{initial} - E_{final} = \frac{RT}{nF} \ln \frac{a_{initial}}{a_{final}} = \frac{RT}{nF} \ln \frac{1}{1-\eta} \qquad (2)$$

Table 2 gives data of ΔE for different values of n and η.

3.1.3 Electrochemical behaviour of the actinide (Th) and the lanthanides (Nd, Gd and Sm):

Thorium system

Figure 1 shows the cyclic voltammogram of the LiF-CaF_2-ThF_4 melt using a Mo electrode.

On this electrode, thorium ions are reduced at a potential of around -1.6 V versus the quasi reference electrode (QRE) in a single step exchanging 4 electrons and thus obviously yielding thorium metal. The reduction potential of thorium ions is significantly far from that of the solvent (ΔE around 0.5 V).

The influence of the potential scan rate on the cyclic voltammetry results is examined in figure 2. The cathodic peak intensity is correlated with the square root of the potential scanning rate by either the Randles Sevcik equation, valid for a soluble–soluble system, or the Berzins-Delahaye equation valid for a soluble-insoluble system [7].

As shown in figure 2, where .we observe that the linearity of peak current density versus the square root of potential scanning rate is verified, the electrochemical process is controlled by the diffusion of the Th^{IV} ions in solution.

Neodymium system [8, 9]

Figure 3 shows the cyclic voltammogram of a melt containing neodymium using a Ta electrode.

It can be observed that neodymium ions are reduced at a potential of around -1.85 V versus the QRE in a single step exchanging 3 electrons giving neodymium metal. The difference between the potential reduction of Nd^{III} ions and of the solvent is around 0.25 V. This low difference is in agreement with the thermodynamic calculations (see table1).

According to table 2, the theoretical extraction of Nd from the solvent should reach between 99.9% and 99.99%. As in the case of Th system, according to ref. [9], the electrochemical reduction process is controlled by the diffusion of Nd^{III} ions in the melt.

Gadolinium system

Figure 4 exhibits the cyclic voltammogramm of a melt containing gadolinium for a molybdenum electrode: Gadolinium ions are reduced in one step into metal at a potential around -1.91 V referred to the QRE. The number of exchanged electrons during the reduction process being found equal to 3, it can be concluded that the product of the reaction is gadolinium metal. The difference of potential between Gd^{III} and the reduction of the solvent is too small (less than 0.17 V) suggesting that, according to the data in table 2, less than 99.9% of Gd extraction can be expected in this medium.

Samarium system [10]

The cyclic voltammogram of the melt containing samarium using a Mo electrode, shown in figure 5, exhibits only one peak in the cathodic run at -1.3 V versus the QRE before the reduction of the solvent. The number of exchanged electrons during this reaction is found to be one and so corresponds to the reduction of Sm^{III} into Sm^{II}. As predicted by thermodynamic data, the reduction of Sm^{II} into metal was not observed on this cyclic voltammogram at potentials more positive than that of solvent reduction. Consequently, as for the thorium system, the electrochemical reduction process in this step is controlled by the diffusion of Sm^{III} ions in the melt.

According to these results, presented in more detail in ref. [10], it can be concluded that the extraction of samarium from the fluoride melt is impossible on an inert cathode.

3.1.4 Discussion

Table 3 gathers the values of ΔE calculated using the cyclic voltammetry results, differences between the electrodeposition potential of the elements to separate (Th-Nd) and elements to extract from the solvent (Nd, Gd and Sm).

We have noticed the good agreement of these results with thermodynamic ones which can be calculated using data from table I. Comparing them to table 2 dealing with the minima of calculated ΔE required for a complete separation or extraction, we can conclude that, on an inert cathode, the separation Th-Nd should be achieved with a satisfactory extraction level (between 99.9% and 99.99%) the extraction of lanthanides from the solvent should not be complete.

These results were confirmed by the cyclic voltammogram shown in Figure 6 of a fluoride melt containing both ThF_4 and NdF_3 where it can be observed that the difference of reduction between Th^{IV} and Nd^{III} ions (0.25V) is less than the minimum value of 0.29 V, given in table 3.

Thus, according to these data, the separation of thorium from neodymium should be possible by electrodepositing thorium with an extraction yield of 99.9% to 99.99%. As neodymium is the least reactive of the Ln elements, its extraction in the presence of other lanthanides such as Sm and Gd should be higher than 99.99%.

The results obtained here prove that the extraction of Ln in a pure metallic form on an inert cathode should only be possible with an insufficient extraction yield (Nd, Gd) or thermodynamically impossible (Sm).

3.2 Electrodeposition on a reactive cathode: nickel

3.2.1 Introduction

A judicious way to increase the separation rate of the different species from the molten mixture should be to decrease the activity of the electrodeposited metal. That can be possible

if the electroreduction of the ions concerned leads to the formation of alloys with the cathodic substrate.

In the case where the cathodic metal reacts with the electrodeposited metal to form an intermetallic compound, the equilibrium potential is shifted in the anodic direction. This depolarisation effect is obviously associated with the lowering of the activity of the electrodeposited metal alloyed with the cathodic substrate.

The methodology was fully developed and explained in our laboratory in ref. [11] and in another work [12] while ref. [13] deals with examples from the literature where this approach was used for the preparation of new materials.

Nickel seemed to be a good candidate for such a cathode metal, since in previous works, it was shown that alloying nickel with a rare-earth element by electrodeposition is easy and rapid at moderate temperatures [14, 15].

In the following part of the present work, we attempt to correlate the phase diagrams of the binary system Ni-Ln with the cyclic voltammograms on a nickel electrode in order to verify the formation of alloys of the electrodeposited element with nickel at more anodic potential and to identify these alloys.

3.3.2 Binary diagrams of Ln-Ni systems

According to the different phase diagrams for Ni-Nd, Ni-Gd and Ni-Sm systems respectively (Binary Alloy Phase Diagrams, second ed. ASM International, 1996), it can be noted that the elements considered are slightly soluble in nickel (phase α between Ni and each element). This low solubility promotes the diffusion process leading to various intermetallic compounds.

The diagrams of Ln-Ni systems exhibit liquid intermetallic compounds in the temperature range of the experiments and in the part of the diagram with high Ln content. Furthermore, the eutectic compositions of these compounds exhibit a particularly low melting point. In

contrast, we observe that the phases with high nickel content have a melting point above the temperature range of the experiments.

3.2.3 Electrochemical behaviour of the studied lanthanides on the reactive electrode

Figures 7a, 7b and 7c compare the cyclic voltammograms of fluoride melt containing lanthanides obtained on inert electrodes (Mo or Ta) and the reactive nickel electrode for Nd, Gd and Sm.

First, the cyclic voltammograms of the samarium system (figure 7c) exhibit on nickel the same reduction wave, corresponding to the Sm^{III}/Sm^{II} system, as on molybdenum.

Likewise, in figures 7a and 7b, the reduction of Nd^{III} and Gd^{III} to pure metal is also observed to occur at the same potential as on inert electrodes.

Then, it can be observed in each of these figures that, on the nickel electrode, additional waves appear prior to the reduction of these ions to give pure metal on Mo substrate. The samarium system also exhibits the same type of waves before solvent reduction. All these waves are attributed to the formation of Ln-Ni alloys.

In each case, the potentiąl gap between the most anodic of these waves likely associated to the formation of lanthanide alloys and solvent reduction are around 0.65, 0.70 and 0.65 V for Nd, Gd and Sm respectively. This suggests that the extraction of the lanthanide from the solvent by alloy formation with nickel should be clearly more efficient than the formation of pure metal on an inert electrode.

3.2.2 Electrolysis performed on a nickel cathode

In order to verify the feasibility of the formation of the alloys, by means of the electrochemical reduction of each element investigated on a reactive substrate, as predicted above, several electrolysis runs were performed on a nickel cathode for each lanthanide. The

runs were performed at constant current at a potential less positive than on an inert cathode and so corresponding to the alloy formations observed on the cyclic voltammograms.

Cross sections of the electrodes obtained after the runs were observed by scanning electron microscopy and EDS probes allowed us to determine the composition of each phase present on the micrograph.

Figures 8a, 8b and 8c show cross sections of a nickel electrode after reduction of Nd^{III}, Gd^{III} and Sm^{III} respectively, for 1 or 2 hours at temperatures around 850°C. The coating is seen to be made up of Ln-Ni alloys. The EDS analyses showed that:

- In each case, intermetallic diffusion leads to compounds with a high nickel content. Each layer is composed of two phases (Ni_2Nd, Ni_3Nd; $GdNi_2$, GdNi; Ni_2Sm, Ni_3Sm).
- In figures 8a and 8b, (respectively Nd-Ni and Gd-Ni systems), the distribution of the phases is coarse whereas in figure 8c, it can be observed that the distribution of Ni_2Sm and Ni_3Sm is thinner and suggesting a demixing effect.

Note that part of the coating fell to the bottom of the crucible, proving that the intermetallic diffusion leads to the formation of liquid intermediates.

Each of these figures illustrates the significant thickness of the alloy layer obtained following the short duration of the electrolysis run. This suggests that the extraction of lanthanides from the fluoride melt by electrodeposition on a nickel cathode should be a high rate process.

3.2.3 Discussion

When performed on a reactive nickel electrode, the electroreduction of all the lanthanides studied in this work was observed with a strong depolarisation effect compared to an inert cathode. This is due to the decrease of the metal activity by alloy formation with the Ni substrate. The gain, in terms of ΔE between the formation of the first lanthanide alloys and the

solvent reduction (ΔE Ln-solvent) is obviously enough for complete separation. The values of ΔE reported in table 4 and compared with the theoretical values of table 2 confirm this assumption.

4 Concluding remarks

This study allows us to conclude that the reprocessing of molten fluorides by electrochemical reduction process on an inert cathode is feasible for the separation of thorium from the melt with a high efficiency. It is not expected that lanthanide-solvent separations could occur at high yield in similar conditions.

Nevertheless, recycling the solvent by electrochemical extraction of lanthanides proves to be satisfactory with the use of a reactive nickel cathode, and is promising for nuclear waste treatment.

The electrochemical process for separation or extraction of Ln-solvents on a reactive nickel electrode presents two major advantages:

- First, the diffusion of Ln inside the nickel substrate is a fast process.
- Secondly, all the Ln-Ni intermetallics with high Ln contents can be obtained in liquid form at a moderate temperature.

The follow-up of this study will consist in: (i) determining the rate of separation by electrochemical reduction processes on nickel electrodes of each Ln element in the melt; (ii) the design of the electrochemical reactor for the separation of thorium from lanthanides.

Acknowledgments

This project was partly funded by CEA Valrho-Marcoule (A. Laplace) and EDF Clamart (E. Walle) for the neodymium studies and by the PACE Program (GDR PARIS and PCR RSF Thorium) from CNRS.

References

[1] H. G. MacPherson, Nucl. Sci. Eng., 90 (1985) 374.

[2] P. Chamelot, P. Taxil and B. Lafage, Electrochim. Acta, 39 (17) (1994) 2571

[3] L. Massot, P. Chamelot, F. Bouyer and P. Taxil, Electrochim. Acta, 47 (12) (2002) 1949.

[4] Y. Bergouthe , A. Salmi, F. Lantelme , J. Electroanal. Chem., 365 (1994) 171.

[5] Barin I., Thermochimical data of pure substances, VCH Verlags Gesellschaft, Weinheim (1989).

[6] Barin I, Thermochimical data of pure substances, Part I and Part II, VCH Verlags Gesellschaft, Weinheim, (1993).

[7] A. J. Bard and R. L. Faulkner, Wiley Ed., New York, 1980.

[8] E. Stefanidakis, C. Hasiotis, C. Kontoyannis, Electrochim. Acta 46 (2001) 2665.

[9] C. Hamel, P. Chamelot and P. Taxil , Electrochim. Act., 49 (2004) 4467.

[10] L. Massot, P. Chamelot and P. Taxil, Electrochim. Acta, 50(28) (2005) 5510.

[11] P. Taxil, J. of the Less-common Metals, 113 (1985) 89.

[12] W. Weppner and R. A. Huggins, J. Electrochem. Soc., 124 (1977) 1569.

[13] P. Taxil, P. Chamelot, L. Massot, C. Hamel, J. Min. Metall.Sec. B:Metall. 39 (2003) 177.

[14] G. Picard ., Y. E. Mottot and B. L. Tremillon, Proc. 4th Int. Symp.on Molten Salts, San Francisco, (1983).

[15] Yamamoto H., Kuroda K., Ichini R. and Okido M., Electrochemistry (Tokyo), 68 (7) (2000) 5914.

Legends of figures and Tables:

Figure 1 Cyclic voltammogram of LiF-CaF_2-ThF_4 (5.20 10^{-2} mol.kg^{-1}) system at 0.1 V/s and T=840 °C. Electrode: Ta.

Figure 2 Linear relationship of ThF_4 peak current density versus the square root of the scanning potential rate, T =840 °C. Electrode: Ta.

Figure 3: Cyclic voltammograms of LiF-CaF_2-NdF_3 (1.00 10^{-1} mol.kg^{-1}) system at 0.1 V/s and T =840 °C. Electrode: Ta.

Figure 4: Cyclic voltammograms of LiF-CaF_2-GdF_3 (2.10 10^{-1} mol.kg^{-1}) system at 0.1 V/s and T =840 °C. Electrodes: Mo.

Figure 5: Cyclic voltammograms of LiF-CaF_2-SmF_3 (2.53 10^{-1} mol.kg^{-1}) system at 0.1 V/s and T =840 °C. Electrodes: Mo.

Figure 6 Cyclic voltammogram of LiF-CaF_2-ThF_4 (7.76 10^{-2} mol.kg^{-1})-NdF_3 (2.05 10^{-1} mol.kg^{-1}) system at 0.1 V/s and T =840 °C. Electrode: Ta.

Figure 7a: Cyclic voltammograms of LiF-CaF_2-NdF_3 (9.80 10^{-2} mol.kg^{-1} mol.kg^{-1}) system at 0.1 V/s and T =840 °C. Electrodes: Ni or Mo.

Figure 7b Cyclic voltammograms of LiF-CaF_2-GdF_3 (2.10 10^{-1} mol.kg^{-1}) system at 0.1 V/s and T =840 °C. Electrodes: Ni or Mo.

Figure 7c Cyclic voltammograms of LiF-CaF_2-SmF_3 (2.53 10^{-1} mol.kg^{-1}) system at 0.1 V/s and T =840 °C. Electrodes: Mo or Ni.

Figure 8a: SEM micrograph of the cross section of a nickel plate after reduction of NdF_3 at 35 mA.cm^{-2} and 840°C for 2 hours.

Figure 8b: SEM micrograph of the cross section of a nickel plate after reduction of GdF_3 at 32 mA.cm^{-2} and 840°C for 2 hours.

Figure 8c: SEM micrograph of the cross section of a nickel plate after reduction of SmF_3 at 35 $mA.cm^{-2}$ and 850°C for 1 hour.

Table 1 Properties of several electrolytic baths. Comparison between the reduction potential of the solvent cations and the reduction potential of the studied species. Reference of potential: F_2/F^- at T=1100 K.

Table 2: theoretical gap potential calculated at 1100 K necessary for fixed extraction efficiency and number of electrons exchanged.

Table 3: experimental difference of potential of considered actinide –lanthanide and lanthanide-Li based solvent on inert (Mo or Ta) electrode.

Table 4: experimental difference of potential of considered actinide –lanthanide and lanthanide-Li based solvent on reactive nickel electrode.

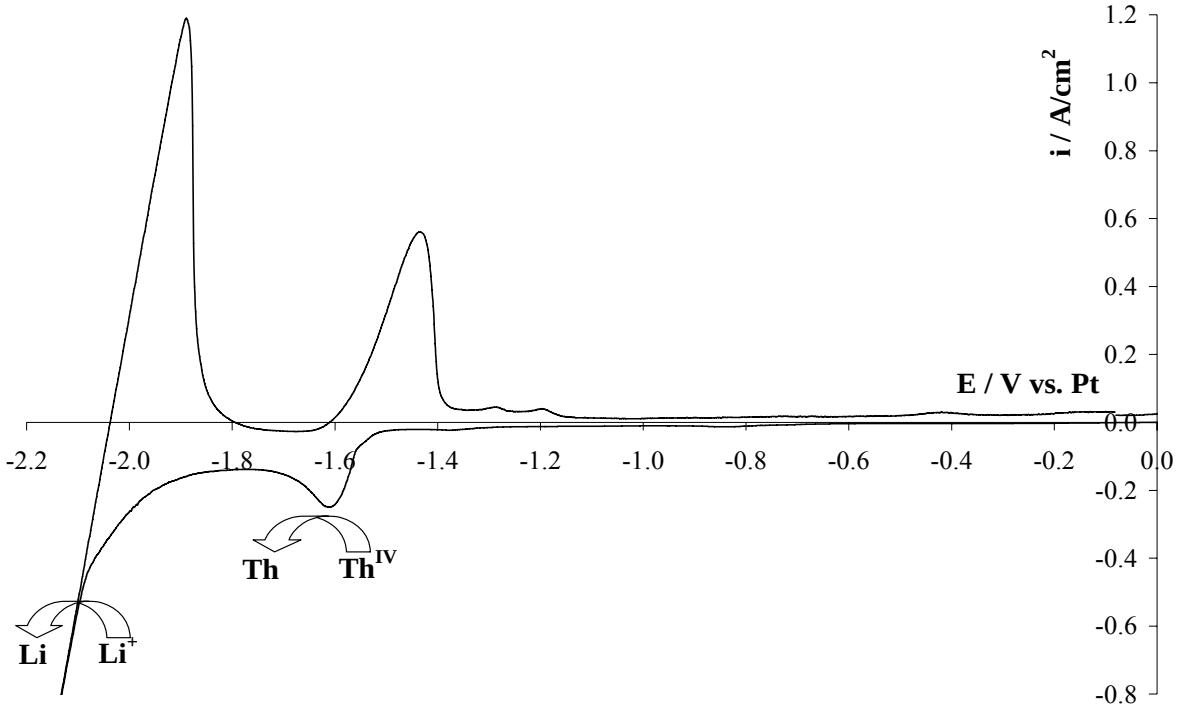
1.2
1.0
0.8
0.6
0.4
0.2
0.0
-0.2
-0.4
-0.6
-0.8
i / A/cm2
E / V vs. Pt
-2.2
-2.0
-1.8
-1.6
-1.4
-1.2
-1.0
-0.8
-0.6
-0.4
-0.2
0.0
Th
ThIV
Li
Li+

Figure 1

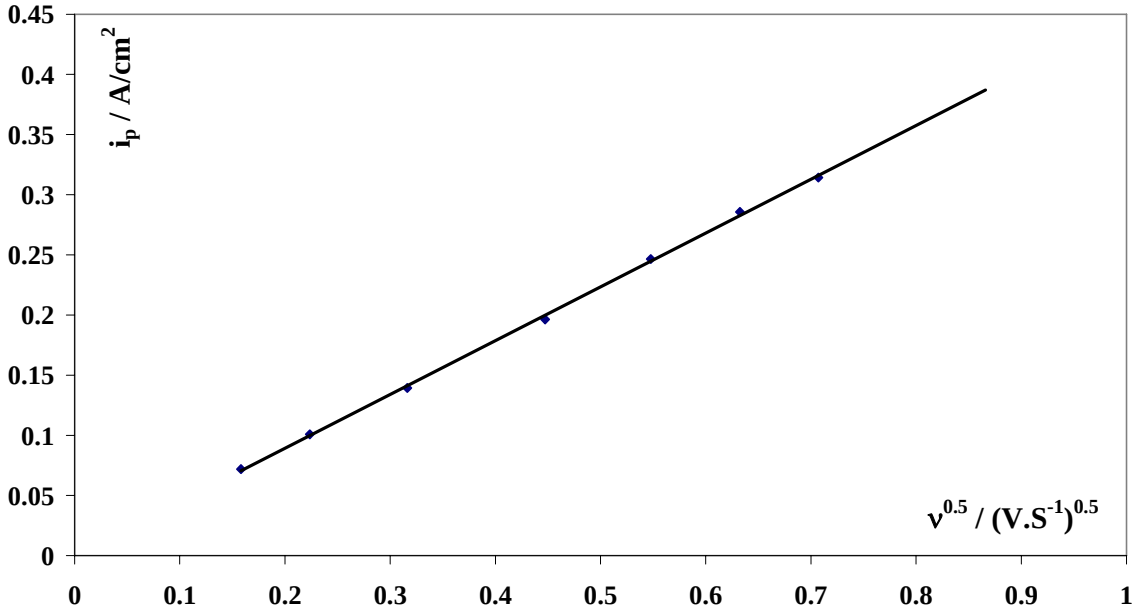
0.45
0.4
0.35
0.3
0.25
0.2
0.15
0.1
0.05
0
i_p / A/cm^2
0
0.1
0.2
0.3
0.4
0.5
0.6
0.7
0.8
0.9
1
$\nu^{0.5}$ / (V.S^{-1})$^{0.5}$

Figure 2

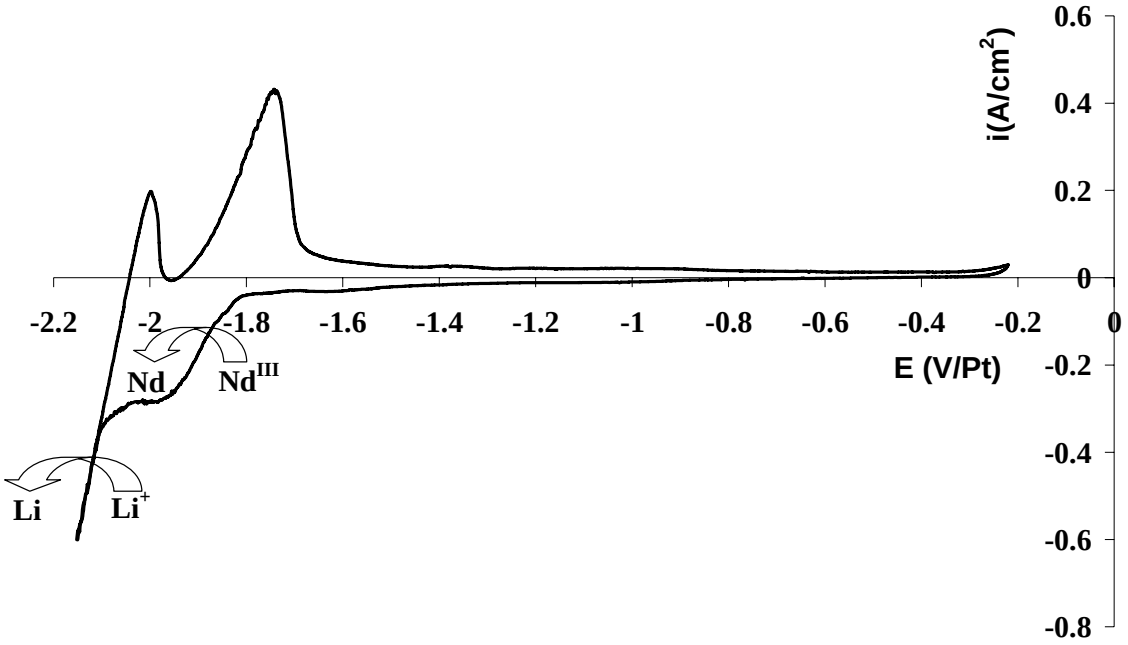
0.6
0.4
0.2
0
-0.2
-0.4
-0.6
-0.8
i(A/cm2)
-2.2
-2
-1.8
-1.6
-1.4
-1.2
-1
-0.8
-0.6
-0.4
-0.2
0
E (V/Pt)
Nd
NdIII
Li
Li+

Figure 3

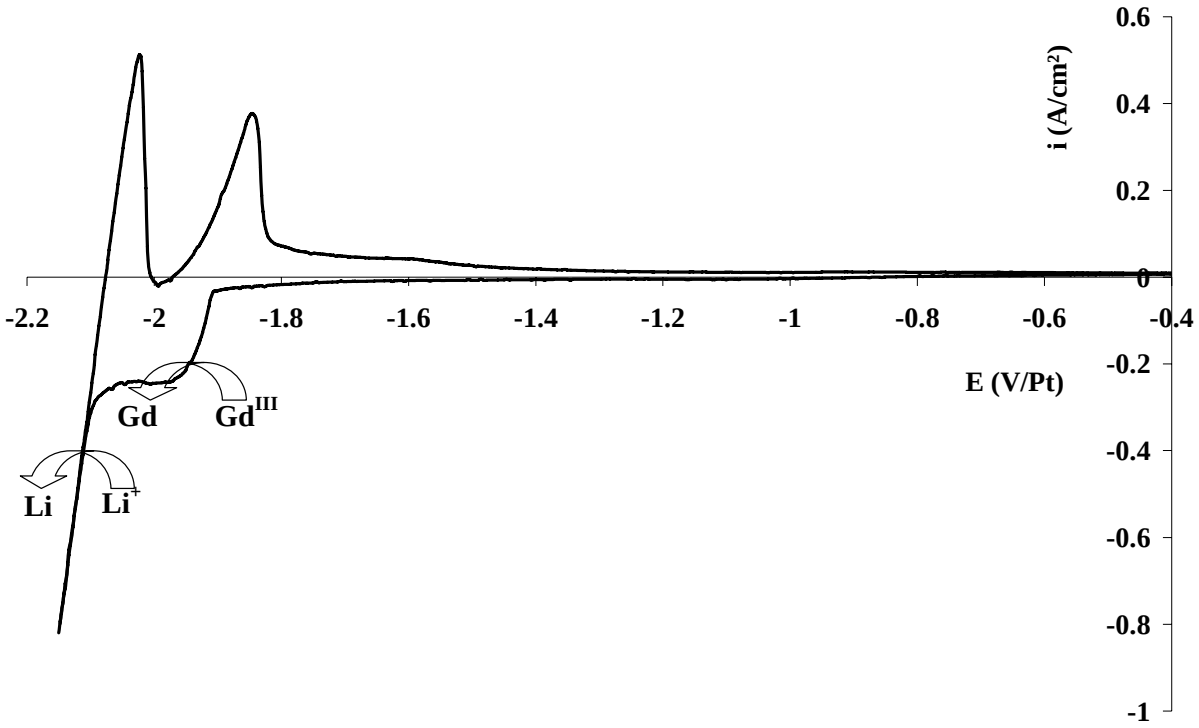
0.6
0.4
0.2
0
-0.2
-0.4
-0.6
-0.8
-1
i (A/cm²)
-2.2
-2
-1.8
-1.6
-1.4
-1.2
-1
-0.8
-0.6
-0.4
E (V/Pt)
Gd
Gd^III
Li
Li+

Figure 4

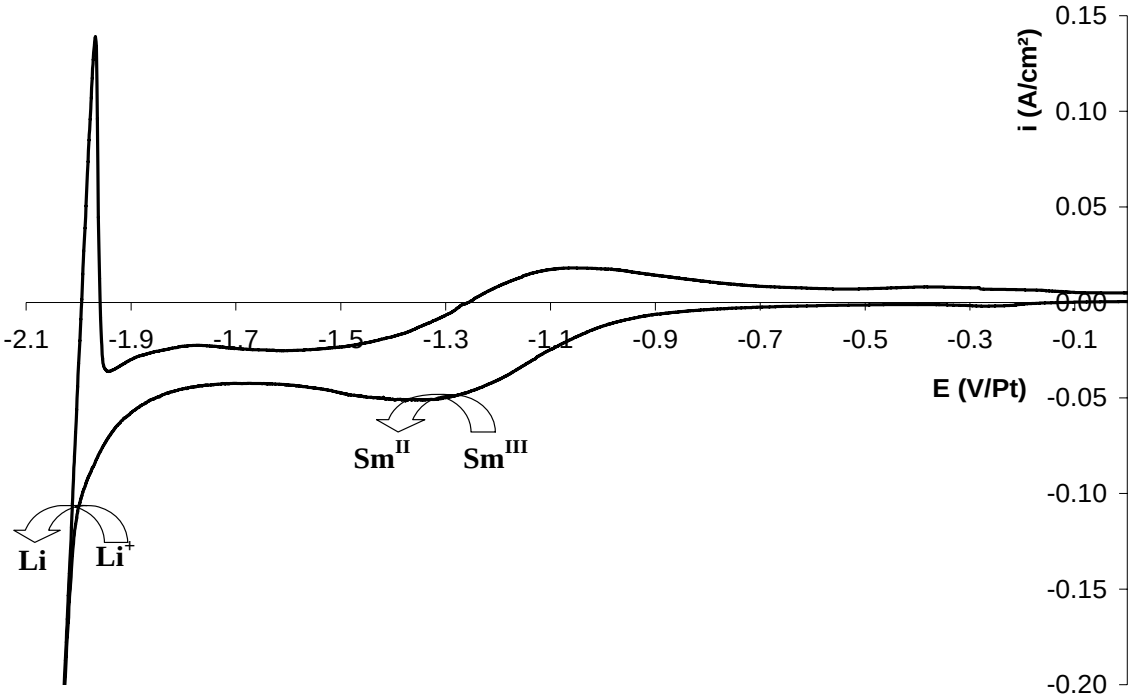
0.15
0.10
0.05
0.00
-0.05
-0.10
-0.15
-0.20
i (A/cm²)
-2.1
-1.9
-1.7
-1.5
-1.3
-1.1
-0.9
-0.7
-0.5
-0.3
-0.1
E (V/Pt)
Li
Li+
SmII
SmIII

Figure 5

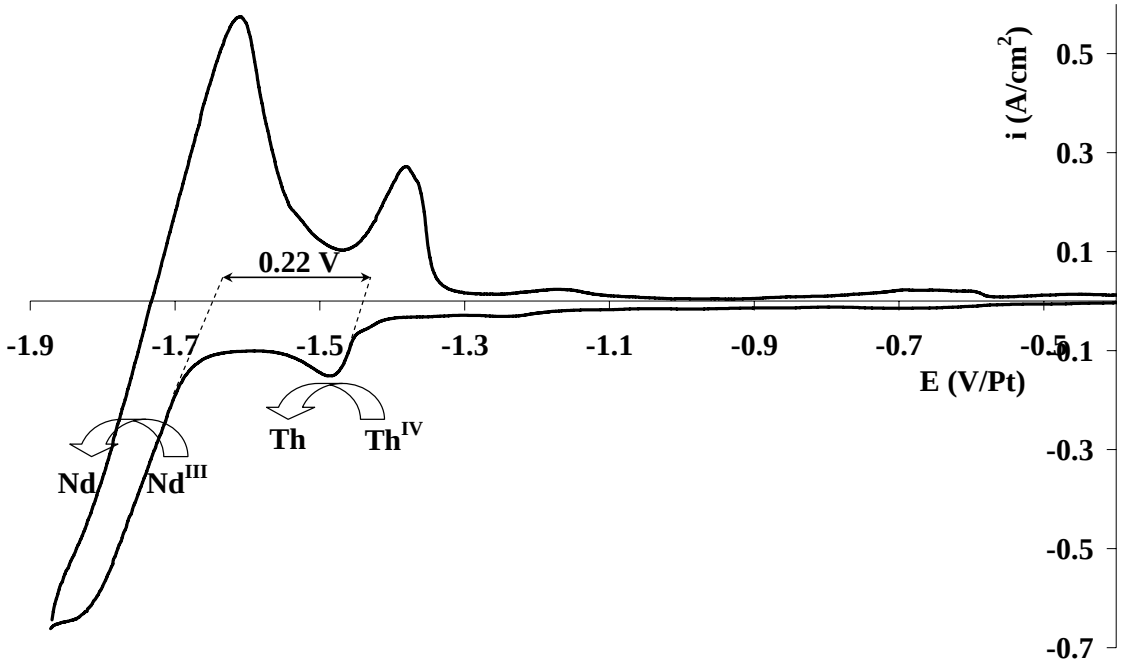
i (A/cm2)
0.5
0.3
0.1
-0.1
-0.3
-0.5
-0.7
0.22 V
-1.9
-1.7
-1.5
-1.3
-1.1
-0.9
-0.7
-0.5
E (V/Pt)
Nd
NdIII
Th
ThIV

Figure 6

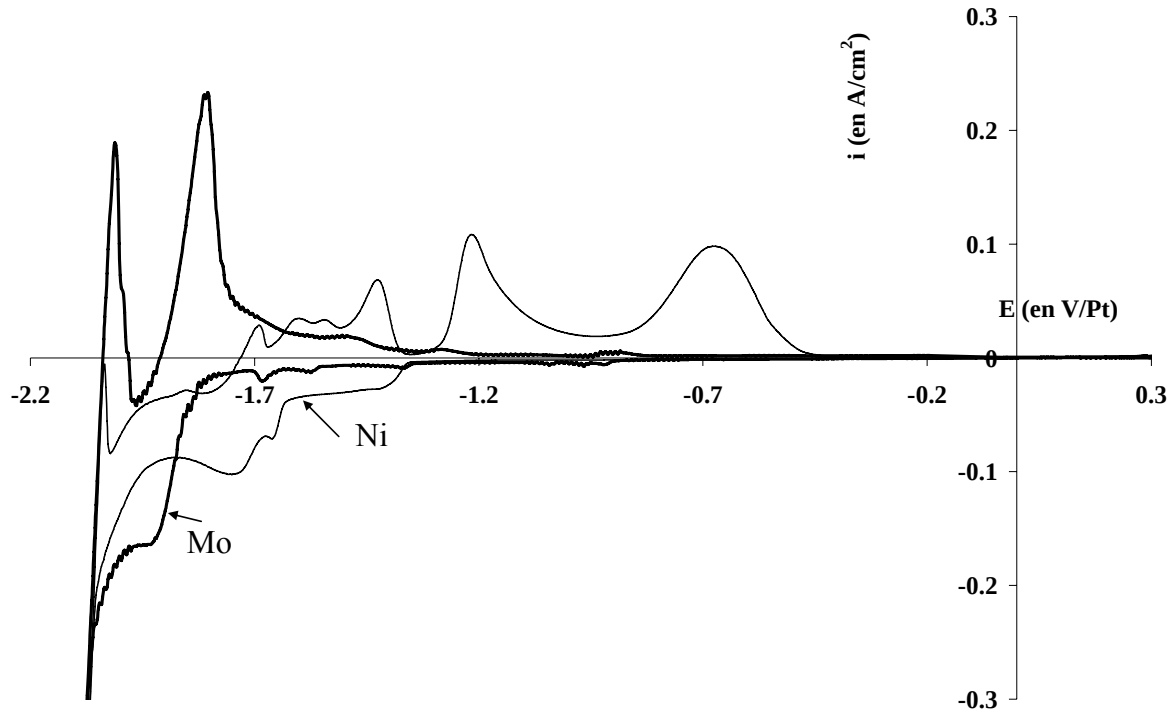

Figure 7a

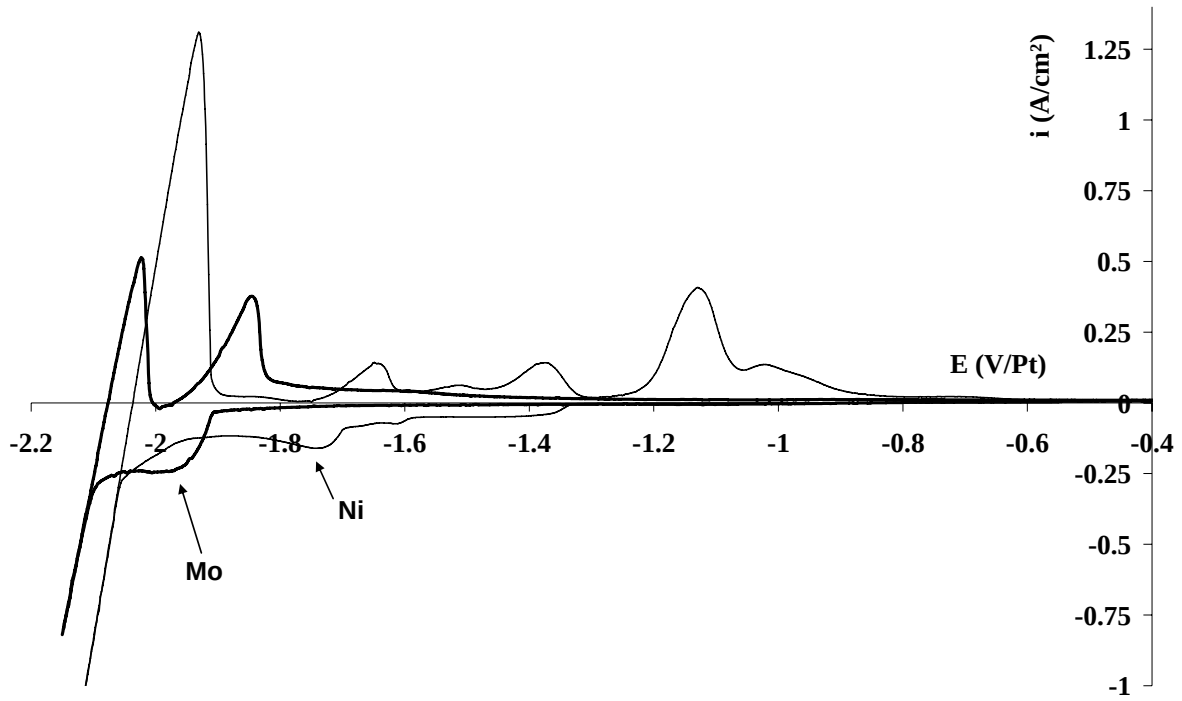
i (A/cm²)
1.25
1
0.75
0.5
0.25
0
-0.25
-0.5
-0.75
-1
E (V/Pt)
-2.2
-2
-1.8
-1.6
-1.4
-1.2
-1
-0.8
-0.6
-0.4
Ni
Mo

Figure 7b

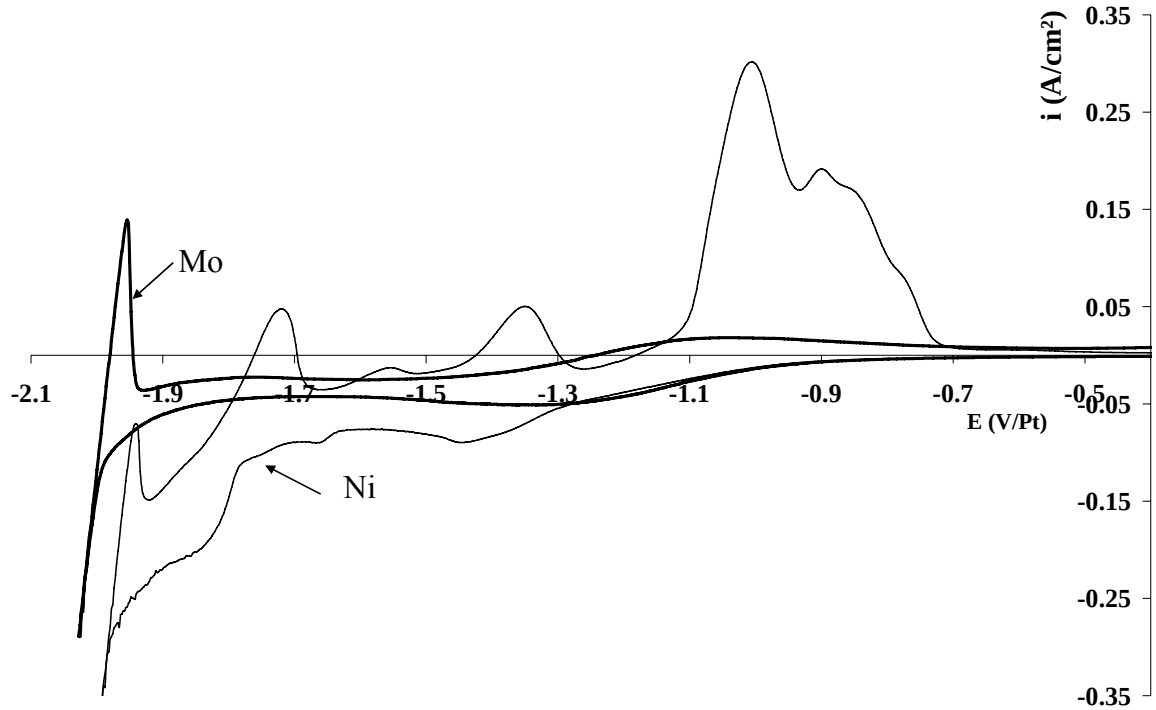
i (A/cm²)
0.35
0.25
0.15
0.05
-0.05
-0.15
-0.25
-0.35
-2.1
-1.9
-1.7
-1.5
-1.3
-1.1
-0.9
-0.7
-0.5
E (V/Pt)
Mo
Ni

Figure 7c

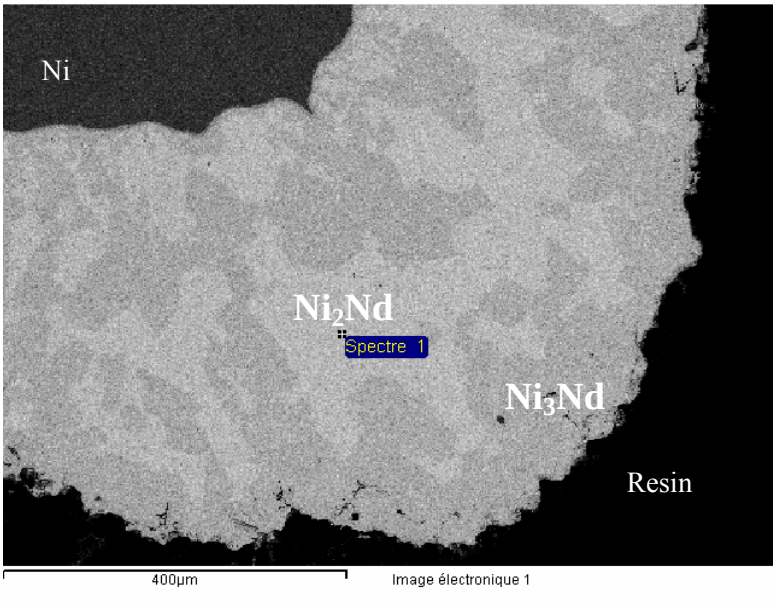

Figure 8a

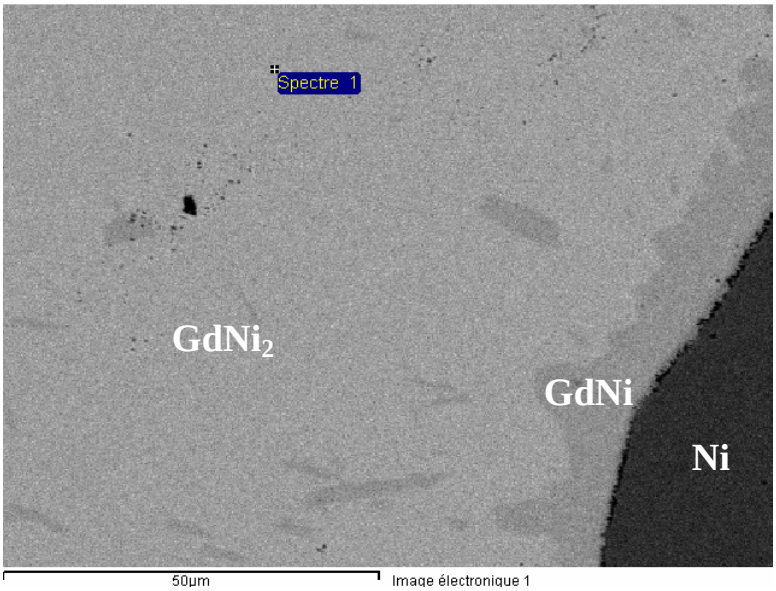

Figure 8b

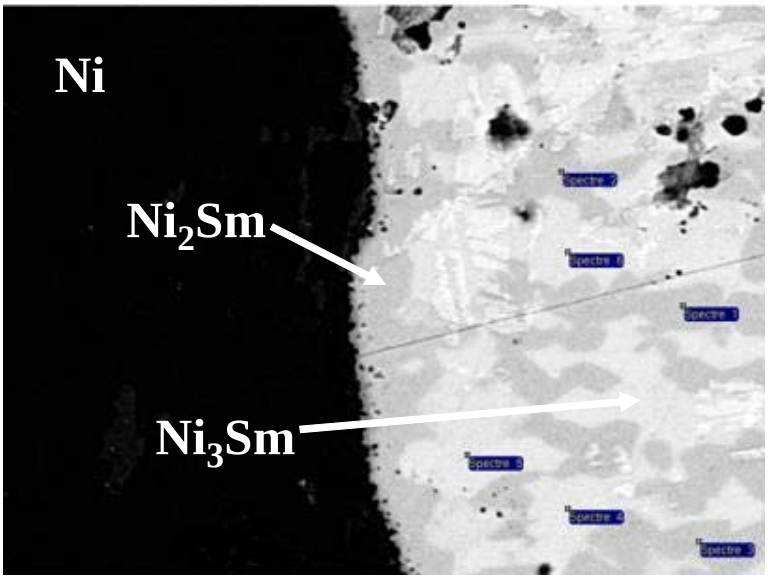

Figure 8c

	$LiF-CaF_2$	LiF	LiF-NaF	LiF-KF	$LiF-BeF_2$	ThF_4	NdF_3	SmF_3	GdF_3
Molar%	77-23	100	64-40	50-50	67-33				
Melting Point	760°C	846°C	652°C	495°C	732°C				
E_{red} (V vs Ref)	-5.33	-5.31	-4.88	-4.81	-4.52	-4.57	-4.88	-5.58*	-4.93

Table 1:

	99%	99.9%	99.99%	99.999%
ΔE n=2 (V)	0,22	0,33	0.44	0.55
ΔE n=3 (V)	0,15	0,22	0.29	0.36
ΔE n=4 (V)	0,11	0,17	0.22	0.27

Table2

	ΔE (Th-Nd)	ΔE (Nd-Solvent)	ΔE (Sm-Solvent)	ΔE (Gd-Solvent)
Inert electrode (Mo or Ta)	~ 0.25 V	~ 0.25 V	---	~ 0.17 V

Table 3

	ΔE (Nd-Solvent)	ΔE (Sm-Solvent)	ΔE (Gd-Solvent)
Reactive electrode: Ni	~ 0.65 V	~ 0.65 V	~ 0.70 V

Tableau 4